

## FROM DYNAMIC MECHANICAL PROPERTIES TO PLASTIC STRAIN BEHAVIOR OF EPOXY NETWORKS. EFFECT OF THE NETWORK ARCHITECTURE

A. Pierre<sup>1</sup>, O. Sindt<sup>2</sup>, N. Thorne<sup>3</sup>, J. Perez<sup>2</sup>, and J.F. Gérard\*<sup>1</sup>

<sup>1</sup> UMR CNRS #5627, Laboratoire des Matériaux Macromoléculaires, INSA Lyon, Bât. 403, 69621 Villeurbanne Cedex, France

<sup>2</sup> GEMPPM INSA Lyon, Bât. 502, 69621 Villeurbanne Cedex, France

<sup>3</sup> Centre de Recherches CRV, Péchiney Co., Centralp, 38340 Voreppe, France

**SUMMARY:** Closed epoxy networks with various architectures, i.e., crosslink density and chain flexibility between crosslinks, were considered in this study. The crosslink density can be varied by preparing epoxy-amine networks from a mixture of primary amines having different functionalities using mixtures of poly(oxypropylene)amines or a monofunctional amine having the same chemical structure acting as a chain extender. The chain flexibility is modified by considering aliphatic epoxy prepolymers instead of aromatic. The influence of the architecture of the epoxy networks on the low- and high-stress mechanical properties is discussed. The dynamic mechanical spectroscopy conducted in wide ranges of frequency and temperature gives insight into the molecular level analyzing the data in both the glass transition region ( $\alpha$ -relaxation) and sub- $T_g$  relaxation zones. A model described by Perez and based on the existence of nanofluctuations of density or quasi-point defects and the concept of hierarchically correlated molecular motions are also used to describe the low-stress mechanical behaviour. The same theory is extended by taking into account the large-stress effects and used to analyze the stress-strain curves recorded in compression at various temperatures and strain rates. This modeling can describe variation of the flow stress with temperature and gives a unique description of the yielding of all the epoxy networks. From this model, the main physical parameter determining the flow stress is the cohesion of the solid state resulting from intermolecular interactions; the loss of cohesion, as temperature increases, corresponds to the  $\alpha$ -process which depends on the network architecture. Finally, the strain and stress at break ( $\sigma_r$  and  $\epsilon_r$ ) recorded in tension at various temperatures and strain rates for epoxy networks having various crosslink densities are correlated with the low-stress behavior from the shift factors,  $a_T$ , determined in the glass transition region.

### Introduction

Thermoset polymers, in particular epoxies, are well known in industrial applications such as matrices for composite materials, structural adhesives, or coatings. These polymers show a low toughness compared with that of thermoplastics; in most cases, their fracture resistance increases by adding a second phase such as a high- $T_g$  thermoplastic or a functionalized

elastomer (1-3). One of the main fracture mechanisms involved in the toughening of polymer blends based on thermosets is the shear yielding of the thermoset network (4,5).

In order to check the ability of various theories developed in the literature to describe the yielding of epoxy networks, the architecture of the network determined by the initial chemistry was changed. The architecture can be changed in different ways modifying the flexibility and/or the molar mass of the chains between crosslinks. Numerous papers reported such changes caused by: (i) substitution of aromatic epoxy and/or amine comonomers for aliphatic ones; (ii) use of mixtures of amine comonomers having different functionalities (in particular, the use of a primary amine which acts as a chain extender); (iii) changes in the length of the epoxy prepolymer (6-10). Cure schedules leading to an incomplete conversion of functional groups and stoichiometric ratios different from unity were also used. In this case, the effects of the presence of dangling chains and unreacted species can also interfere with the mechanical response.

The aim of this paper is to describe the effect of the network architecture of epoxy networks on the low- and high-amplitude mechanical behavior. A molecular model, previously developed by Perez, is used to propose a unique description of the yielding behavior of epoxies and to determine main parameters governing mechanical properties of thermoset networks.

## Experimental

### *Epoxy networks*

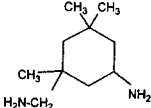
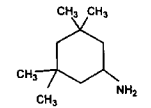
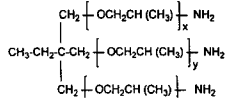
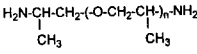
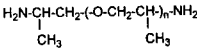
Two types of epoxy networks synthesized from the reactants described in Table 1 are considered in this study. For all the epoxy networks, the stoichiometric (epoxy-to-amino hydrogen) ratio was equal to unity and the cure schedules were chosen in order to ensure that the glass transition temperature ( $T_{g\infty}$ ) is maximum. Thus, the epoxy networks are closed, i.e., they have no dangling chains.

The first series of networks were synthesized from an aromatic or aliphatic diepoxide (DGEBA-DER332 from Dow Chemicals,  $n = 0.03$ , or DGEBD, respectively) and a tetrafunctional amine, 1,5,5-trimethylcyclohexane-1,3-diamine or isophoronediamine (IPD; from Hüls). A network was also prepared from a mixture of IPD and a difunctional amine, 1,3,3-trimethylcyclohexylamine (TMCA), the latter acting as a chain extender. For this network, denoted DGEBA/IPD/TMCA, the stoichiometric ratio remained equal to unity, 50 % of the amino groups belonging to TMCA (11).

The second series of epoxy networks considered in this study results from the condensation reaction between DGEBA diepoxide (LY556, Ciba,  $n = 0.15$ ) and a mixture of poly(oxypropylene)amines (Jeffamines T403 and D400, Texaco). The networks are denoted by the percentage of amino functions of the difunctional amine comonomer, i.e. D400 (e.g., for D50, 50 % of the amino groups belong to the diamine) (12).

The molar mass between crosslinks,  $M_c$ , was calculated from molar masses and molar percentages of the comonomers (13). The various reactants are described in Table 1.

Table 1. Reagents used in the synthesis of the epoxy networks

| Reagent                          | Formula   | Molar mass ( $M_n$ )<br>$\text{g mol}^{-1}$ |
|----------------------------------|---|---|
| Bisphenol A diglycidyl ether     | —   | 348.5 (DER332)                              |
| Isophoronediamine                |    | 382 (LY556)                                 |
| 3,3,5,5-Trimethylcyclohexylamine |    | 170.3                                       |
| Jeffamine T403                   |   | 143.1                                       |
| Jeffamine D400                   |  | 439   |
|                                  |   | $x + y + z \approx 5.3$                     |
| Jeffamine D400                   |  | 399   |

### Experimental techniques

The onset glass transition temperature,  $T_g$ , was deduced from differential scanning calorimetry (DSC) measurements. These were performed using a TA3000 calorimeter with 15-mg samples at a heating rate of  $10 \text{ K min}^{-1}$ . The cure schedules leading to a final conversion equal to unity, were checked by performing two consecutive runs in order to verify that there was no exotherm during the first heating and that the  $T_g$  was the same for the two runs.

Dynamic mechanical spectra were obtained using two spectrometers operating in torsion mode, a Métravib spectrometer at a frequency of 1 Hz (leading to dynamic shear modulus,  $G^*$ ) and a Rheometrics RDA2 spectrometer in the frequency range of 0.01 to  $100 \text{ rad s}^{-1}$ . In

both cases, the spectra were recorded from -150 to 50 °C above the  $T_g$  of the networks in order to evidence the secondary and primary mechanical relaxations.

Tensile tests were performed on DGEBA/Jeffamine networks using a Minimat tensile machine on dogbone specimens (20 x 5 x 0.01 mm) with a crosshead speed varying from 10 to 500 mm min<sup>-1</sup> (i.e., from 0.0083 to 0.417 s<sup>-1</sup>) in the temperature range from 30 to 140 °C. Young's modulus, stress and strain at break,  $E$ ,  $\sigma_r$ , and  $\epsilon_r$ , respectively, were obtained from these experiments.

Compression tests were performed using an Adamel Lhomargy tensile machine operating in compression in the temperature range from 143 to 353 K with a crosshead speed of 0.15 mm min<sup>-1</sup>. The specimens were cylinders (diameter 8 mm, height 10 mm). The plastic flow stress,  $\sigma_p$ , was determined and the apparent activation volume,  $V_{exp}$ , was deduced using Guieu and Pratt's equation (13) from stress relaxation recorded after stopping the crosshead as the plastic consolidation was reached. More details were given in a previous paper (11).

## Discussion

Figure 1 shows dynamic mechanical spectra of some epoxy networks considered in this study.

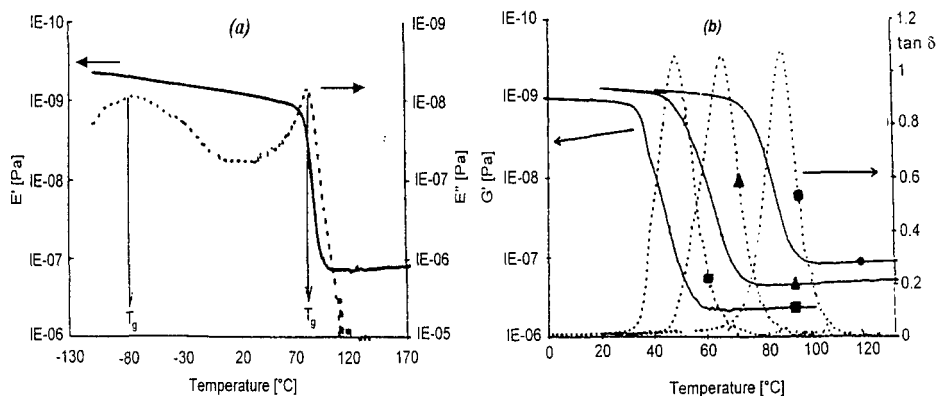


Figure 1. Dynamic mechanical spectra in the main relaxation zone for DGEBA/Jeffamine networks at 1 Hz: (a) storage and loss moduli,  $E'$  and  $E''$ , (b) storage modulus  $G'$  and loss factor,  $\tan \delta$ . (● D0, ▲ D50, ■ D100)

As reported previously, the main relaxation associated with  $T_g$  and denoted  $\alpha$  is evidenced in the glass transition region and a secondary relaxation process, denoted  $\beta$ , is located in the low-temperature region (14,15). From the changes in the storage modulus,  $G'$ , in the  $\alpha$ -relaxation zone and its value on the rubbery plateau, the crosslink density can be evaluated assuming that it obeys the rubber elasticity law (16) and compares with  $M_c$  determined from Bell's equation.

On the basis of NMR experiments in the epoxy-amine networks, the  $\beta$ -process is associated with the motions of the hydroxyether units (17,18). For epoxy networks based on aliphatic diepoxides, a third relaxation, denoted  $\gamma$ , which is associated with the methylene units occurs below  $\beta$  (19). The various relaxation processes in the glassy state can be distinguished on the basis of their apparent activation energies calculated assuming an Arrhenius dependence of the processes on frequency. The main characteristics of the relaxations of the epoxy networks are reported in Table 2 and are in agreement with the data reported in the literature (19-22).

Table 2. Characteristics and molecular relaxations of various epoxy networks

| Network                       | $T_g$<br>°C | $M_c$<br>g mol <sup>-1</sup> | $T_\alpha$ (1Hz)<br>°C | $T_\beta$ (1Hz)<br>°C | $E_\beta$<br>kJ mol <sup>-1</sup> |
|-------------------------------|-------------|------------------------------|------------------------|-----------------------|-----------------------------------|
| <i>Epoxy/IPD/TMCA Series</i>  |             |                              |                        |                       |                                   |
| DGEBA/IPD                     | 163         | 383                          | -                      | -51                   | 54                                |
| DGEBA/IPD 50/TMCA 50          | 110         | 1255                         | -                      | -73                   | 70                                |
| DGEBA/IPD                     | 53          | 350                          | -                      | -46                   | 58                                |
| <i>DGEBA/Jeffamine Series</i> |             |                              |                        |                       |                                   |
| DGEBA/T403                    | 78          | 371                          | 90                     | -78                   | 55                                |
| DGEBA/T403 50/D400 50         | 55          | 655                          | 67                     | -75                   | 56                                |
| DGEBA/D400                    | 38          | 1352                         | 50                     | -78                   | 57                                |

As expected, the value of the storage shear modulus on the rubbery plateau decreases as a primary amine is introduced to the polymer network, i.e., as the crosslink density decreases. Nevertheless, the molar mass between crosslinks cannot be directly compared with the theoretical value as the front factor of the rubber elasticity theory changes with changing flexibility of the chains between crosslinks (22). For diepoxide/IPD/TMCA networks, secondary relaxation processes have a large effect on the storage modulus as a consequence of Young's modulus in the low-temperature region. In fact, Young's modulus at room temperature decreases with increasing crosslink density due to the highest amplitude of the  $\beta$ -peak for higher-crosslinked networks (this effect was denoted as an 'antiplasticization' phenomenon) (23,24).

In DGEBA/Jeffamine networks, the same trends can be reported for changes in the storage modulus on the rubbery plateau. Nevertheless, in contrast to the diepoxy/diamine/monoamine networks, the  $\beta$ -relaxation process is similar for all the networks, i.e., the temperature position, amplitude, and apparent activation energy,  $E_\beta$ , are the same (13). This can be

explained by the fact that the  $\beta$ -process is associated with the motion of hydroxyether moieties which are in the neighborhood of crosslinks in the DGEBA/Jeffamines networks, whereas a part of hydroxyether groups (those resulting from primary monoamines) are far from the crosslinks. The phenomenon that the  $\beta$ -process involves cooperativity was confirmed by analyzing the viscoelastic data using Starkweather's model (25) of the distribution of activation entropy.

As reported previously, Young's modulus measured at room temperature is dependent on secondary relaxation processes. This antiplasticization phenomenon is confirmed by measuring the unrelaxed shear modulus at room temperature and at 10 MHz, i.e., below the  $\beta$ - and  $\gamma$ -relaxation processes. Increasing the flexibility and/or the molar mass between crosslinks induces a decrease in the unrelaxed modulus due to weaker van der Waals intermolecular interactions. In fact, these lead to a lower cohesion and, as the modulus is proportional to second derivative of the interaction energy, it decreases (11).

Epoxy networks undergo a large plastic deformation in compression. The stress-strain curves recorded in compression show common features for epoxy networks (26,27): (i) elastic deformation zone, (ii) stress maximum, denoted  $\sigma_y$ , and (iii) a domain with a constant stress, the plastic flow stress,  $\sigma_p$ , corresponding to plastic consolidation. As the temperature increases, the plastic flow stress decreases (Figure 2).

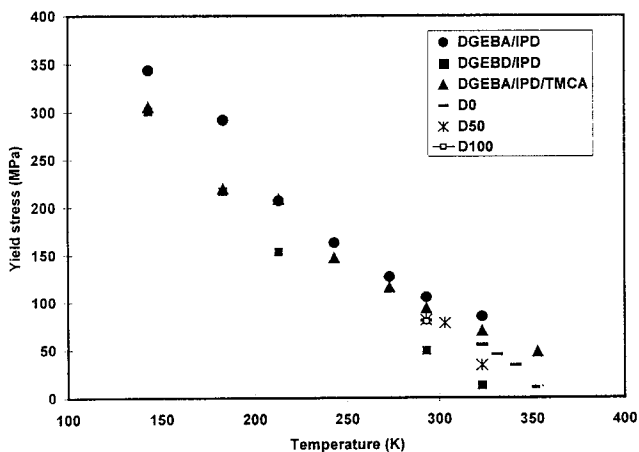


Figure 2.  
Temperature dependence of the yield stress at a strain rate of  $2.4 \times 10^{-4} \text{ s}^{-1}$  for various types of epoxy networks

Different approaches were developed in order to describe the response of a polymer when stress is applied. Eyring's theory of viscous flow was largely used and Bowden and Argon (28) reported a description of the plastic flow at a molecular level. The plastic deformation of epoxy networks was found to be similar to that of glassy thermoplastics and the non-elastic

deformation was described by a plastic shear transformation mechanism (29,30). From a thermodynamic analysis of deformation, Perez developed a theoretical model, which can be used to describe linear and non-linear stress-strain behaviour and which was successfully applied to various amorphous polymers (31,32). This model is based on the existence of nanofluctuations of density or quasi-point defects in the condensed matter. From the concept of hierarchically correlated molecular motions, the mean time for a translational degree of freedom,  $\tau_{\text{mol}}$ , is given by

$$\tau_{\text{mol}} = t_0 \cdot (\tau_1/t_0)^{1/\chi}$$

where  $\tau_1$ ,  $t_0$ , and  $\chi$  correspond to the time of elementary molecular motion, a scaling time, and a measure of constraint of hierarchical molecular entities, respectively.  $\tau_1$  can be identified with the time of secondary relaxations. Finally, Perez's model assumes that the response to an applied stress can be described in terms of thermomechanical relaxation, growth, and coalescence of shear microdomains, resulting in elastic and viscous deformation. As a consequence, the compliance,  $J(t)$ , and the complex shear modulus,  $G^*(i\omega)$ , can be expressed as (11):

$$J(t) = 1/G_u + A \{1 - \exp [-(t/\tau_{\text{mol}})^\chi]\} + A' (t/\tau_{\text{mol}})^{\chi'}$$

$$G^*(i\omega) = G_r + \frac{G_u - G_r}{1 + (i\omega \tau_{\text{mol}})^\chi + Q (i\omega \tau_{\text{mol}})^{\chi'}}$$

where  $G_u$  is the unrelaxed modulus referred to  $\alpha$ -relaxation,  $A$  and  $A'$  are proportionality factors depending mainly on the concentration of defects,  $\chi'$  takes into account the fact that the segmental mobility is affected by the strain above a threshold,  $G_r$  is the relaxed modulus corresponding to the storage shear modulus on the rubbery plateau and the constant  $Q$  is close to unity.

This modeling agrees with the experimental data for low stresses, i.e., from dynamic mechanical spectroscopy (11).  $\chi$  and  $\chi'$  can give insight into the effect of the architecture of the polymer network on molecular motions in the solid state. In fact, for the DGEBA/IPD network,  $\chi'$  is low in agreement with the fact that  $\chi'$  decreases as the chain segments shorten. On the other hand,  $\chi$  also decreases when the number of obstacles, i.e. crosslinks, is maximal, i.e., when these induce a more pronounced hierarchical correlation effect.

The theory, extended to large stress effects on the mechanical response, was used to analyze the compression and relaxation tests. Details of this analysis were given in previous papers (32-34). In this model, the mechanical response of glassy polymers at low temperature, i.e., high stresses, is characterized by an activation volume,  $V_{\text{exp}}$ . This can be determined by stress relaxation measurements performed at the beginning of the plastic consolidation domain and by applying Guiu and Pratt's equations. This volume can be identified as the activation volume related to thermomechanical activation resulting in the elementary molecular motion,  $V_a$ . The modeling leads to the description of the temperature dependence of the flow stress (11). As reported in Fig. 3, various epoxy networks having different chain flexibilities and crosslink densities display the same mechanical behavior, which can be described using Perez's model generalized for large stresses. In this approach, the main parameter governing the flow stress is the cohesion of the solid state resulting from intermolecular interactions. As temperature increases, the loss of cohesion is associated with the main relaxation process which depends on the architecture of the network, i.e., crosslink density, chain flexibility, etc.

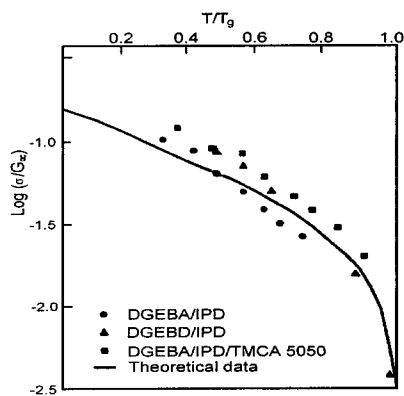


Figure 3. Dependence of the ratio of the yield stress to the unrelaxed shear modulus on temperature at a strain rate of  $7.5 \times 10^{-4} \text{ s}^{-1}$  for various types of epoxy networks. Comparison with the molecular model developed by Perez (Ref. 11).

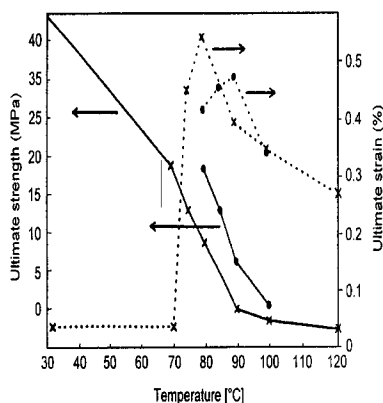


Figure 4. Dependence of the stress and strain at break in tensile tests performed at various temperatures and strain rates for the DGEBA/Jeffamine T403 network. (X 10 mm/min,  $\blacklozenge$  500 mm/min)

For DGEBA/Jeffamine networks, the same trends were found for the changes in the plastic flow with the architecture of networks (35). For example, the plastic flow stress was found to obey Eyring's law with values of activation volume and energy close to those reported in the

literature for epoxy networks (36,37). The mechanical behavior at high stresses was also studied by tensile tests. In this case, the strain and stress at break,  $\epsilon_r$  and  $\sigma_r$ , were recorded as a function of temperature and strain rate (Figure 4). As expected, the transition at high temperature, from glassy to elastomeric behavior, is shifted to high temperatures with increasing the strain rate. In fact, as the temperature increases, Young's modulus and the stress at break decrease whereas the strain at break increases (38,39). In agreement with the literature,  $\epsilon_r$  increases as the molar mass between crosslinks rises (40). The shift factors,  $a_T$ , which can be determined from the strain rate dependence are in agreement with those computed from dynamic mechanical measurements performed at different frequencies in the  $\alpha$ -relaxation zone. These shift factors were used in the literature for constructing master curves from the ultimate strain data recorded at different temperatures and strain rates (41,42).

## Conclusions

Mechanical properties of epoxy networks with various architectures at low and high stress levels can be described by a molecular model previously developed by Perez for linear polymers. The main parameter governing the plastic flow stress is the cohesion of the solid state; its dependence on temperature is related to the main relaxation associated with the glass transition temperature. As a consequence, the flow stress can be related to characteristics of the network such as chain flexibility, length, and molar mass between crosslinks.

Work is in progress verifying this approach on different types of networks, in particular those having permanent heterogeneities, such as microgels, resulting from radical polymerization.

## References

- 1) J. Sultan and F. McGarry, *Polym. Eng. Sci.*, 13, 19 (1973)
- 2) C.B. Bucknall and I.K. Partridge, *Polymer*, 24, 639 (1983)
- 3) R.E. Pearson and A.F. Yee, *J. Appl. Polym. Sci.*, 48, 1051 (1993)
- 4) P.B. Bowden and J.A. Jukes, *J. Mater. Sci.*, 7, 52 (1972)
- 5) E. Oleinik, *Prog. Coll. Polym. Sci.*, 80, 140 (1989)
- 6) V.B. Gupta, L.T. Drzal, and C.Y.E. Lee, *Polym. Eng. Sci.*, 25, 812 (1985)
- 7) J.M. Charlesworth, *Polym. Eng. Sci.*, 28(4), 230 (1988)
- 8) S.C. Misra, J.A. Manson, and L.H. Sperling, in 'Epoxy Resin Chemistry', *Adv. Chem. Ser.* 11, 137 (1979)
- 9) M. Ilavsky, J. Zelenka, V. Spacek, and K. Dusek, *Polym. Networks Blends*, 2, 95 (1992)
- 10) U.M. Vaskil and G.C. Martin, *J. Appl. Polym. Sci.*, 46, 2089 (1992)
- 11) O. Sindt, P. Perez, and J.F. Gérard, *Polymer*, 37, 2989 (1996)
- 12) A. Pierre, N. Thorne, and J.F. Gérard (to be published)
- 13) F. Guieu and P.L. Pratt, *Phys. Status Solidi*, 6, 111 (1964)
- 14) J.F. Gérard, J. Galy, H. Sautereau, and J.P. Pascault, *Synth. Polym. J.*, 1, 175 (1994)
- 15) E. Espuche, J. Galy, J.F. Gérard, J.P. Pascault, and H. Sautereau, *Macromol. Symp.*, 93, 107 (1995)
- 16) L.G.R. Treloar, in 'Physics of Rubber Elasticity', Oxford Univ. Press, 1958

- <sup>17)</sup> T.D. Chang, S.H. Carr, and J.O. Brittain, *Polym. Eng. Sci.*, 22, 1205 (1982)
- <sup>18)</sup> F. Lauprêtre, R.P. Eustache, and L. Monnerie, *Polym. Prep.*, 33(1), 136 (1992)
- <sup>19)</sup> J.M. Charlesworth, *Polym. Eng. Sci.*, 28, 221 (1988)
- <sup>20)</sup> S. Cukierman, J.L. Halary, and L. Monnerie, *Polym. Eng. Sci.*, 31, 1476 (1991)
- <sup>21)</sup> J.H. Schroeder, P.A. Madsen, and R.T. Foister, *Polymer*, 28, 929 (1987)
- <sup>22)</sup> E. Urbacewski, J. Galy, J.F. Gérard, J.P. Pascault, and H. Sautereau, *Polym. Eng. Sci.*, 31, 1572 (1991)
- <sup>23)</sup> Y.G. Won, J. Galy, J.F. Gérard, J.P. Pascault, V. Bellenger, and J. Verdu, *Polymer*, 31, 1787 (1990)
- <sup>24)</sup> Z. Cao, J. Galy, J.F. Gérard, and H. Sautereau, *Polym. Networks Blends*, 4, 15 (1993)
- <sup>25)</sup> H.W. Starkweather, *Macromolecules*, 23, 328 (1990)
- <sup>26)</sup> X. Caux, G. Coulon, and B. Escaig, *Polymer*, 29, 808 (1988)
- <sup>27)</sup> C. G'Sell, D. Jacques, and J.P. Favre, *J. Mater. Sci.*, 25, 2004 (1990)
- <sup>28)</sup> A.S. Argon, *Philos. Mag.*, 28, 839 (1973)
- <sup>29)</sup> I.M. Ward, *J. Mater. Sci.*, 6, 1397 (1971)
- <sup>30)</sup> E.F. Oleinik, O.B. Salamatina, S.N. Rudnev, and S.V. Shenogin, *Polym. Sci.*, 35, 1532 (1993)
- <sup>31)</sup> J. Perez, J.Y. Cavallé, and C. Jourdan, *Rev. Phys. Appl.*, 23, 125 (1988)
- <sup>32)</sup> J. Perez, *Physique et Mécanique des Polymères Amorphes*, Tec Doc. Lavoisier, Paris, 1992
- <sup>33)</sup> M. Mangion, J.Y. Cavallé, and C. Jourdan, *Philos. Mag. A*, 66, 773 (1992)
- <sup>34)</sup> J. Perez and J.M. Lefebvre, *Introduction à la Mécanique des Polymères*, Ed. C. G'Sell, p. 289, INPL, 1995
- <sup>35)</sup> A. Pierre, Ph.D. Thesis, INSA Lyon, 1997
- <sup>36)</sup> A.J. Kinloch, J.C. Shaw, and D.L. Hundson, *Polymer*, 24, 1355 (1983)
- <sup>37)</sup> E. Urbacewski, PhD Thesis, INSA Lyon, 1989
- <sup>38)</sup> J.D. Ferry, *Viscoelastic Properties of Polymers*, 3rd ed., J. Wiley, New York, 1980
- <sup>39)</sup> M. Shimbo, N. Nishitani, and T. Takahama, *J. Appl. Polym. Sci.*, 29, 1709 (1984)
- <sup>40)</sup> M.L.M. van der Sanden, *Polymer*, 34, 5063 (1993)
- <sup>41)</sup> Y. Huang and A.J. Kinloch, *J. Adhesion*, 41, 5 (1993)
- <sup>42)</sup> A.J. Kinloch, *Adv. Polym. Sci.*, 72, 45 (1985)